

Pressure-induced enhancement of two-dimensionality in $\text{LaO}_{1-x}\text{F}_x\text{Bi}(\text{Se/S})_2$ superconductors

V. Svitlyk*¹, A. Krzton-Maziopa², M. Mezouar¹

¹ID27 High Pressure Beamline, European Synchrotron Radiation Facility, 38000 Grenoble, France

²Faculty of Chemistry, Warsaw University of Technology, Noakowskiego 3, 00-664 Warsaw, Poland

*svitlyk@esrf.fr

Abstract

Application of high pressure (HP) induces a metal-semimetal transition in the layered superconducting $\text{LaO}_{1-x}\text{F}_x\text{BiSe}_2$ phase, as concluded from *ab initio* calculations based on experimental P -dependent structural data. These changes in conduction properties are associated with a decrease in the critical ordering temperature, T_c . However, further increase in pressure induces structural transformation in $\text{LaO}_{1-x}\text{F}_x\text{BiSe}_2$ which results in a strong enhancement of its two-dimensionality with the associated improvement in superconducting performance. In addition, the HP structural anisotropy induces a loss of long-range order correlations along the stacking direction of the LaO/F and BiSe_2 layers yielding formation of stacking faults. Similar but even more pronounced structural transition was observed in the related $\text{LaO}_{1-x}\text{F}_x\text{BiS}_2$ phase which is also accompanied by an increase in T_c . This demonstrates that enhancement of two-dimensionality in layered superconducting systems acts in favor of their superconducting performance.

Communication

Layered 2D systems form a major class of superconductive materials with classics like Cu-oxide and Fe-based compounds. Yet another family of layered BiCh_2 -based superconductors (Ch – chalcogenide S or/and Se atoms) have been discovered afterwards ($\text{Bi}_4\text{O}_4\text{S}_3$ ^{1,2}) thus further enriching this vast constellation of 2D superconductive systems. The BiCh_2 -based materials have a typical for layered superconductors structure. Namely, they are composed of conducting BiCh_2 layers which are separated by blocking (spacer) layers which serve as charge reservoirs (Fig. 1, $\text{LaO}_{1-x}\text{F}_x\text{BiSe}_2$ phase is shown). This modular structural arrangement allowed synthesis of numerous derivatives of the parent $\text{Bi}_4\text{O}_4\text{S}_3$ phase,^{3,4} similarly to Cu-oxide and Fe-based systems.

Application of external pressure on the BiCh_2 -based compounds substantially alters their superconducting response. For instance, the $\text{LaO}_{0.5}\text{F}_{0.5}\text{BiSe}_2$ phase with a superconducting transition temperature of about 3 K^{5,6} features a decrease of T_c as a function of pressure^{6,7} (we denote this phase as SCI, $P4/nmm$ symmetry). However, upon a further compression a new phase with an increased $T_c \sim 6$ K emerges (SCII phase).⁶⁻⁸ Emergence of the HP SCII phase was observed in many other BiCh_2 -based materials,⁹⁻¹⁸ including $\text{LaO}_{0.5}\text{F}_{0.5}\text{BiS}_2$.¹⁸⁻²¹ The SCII phase was

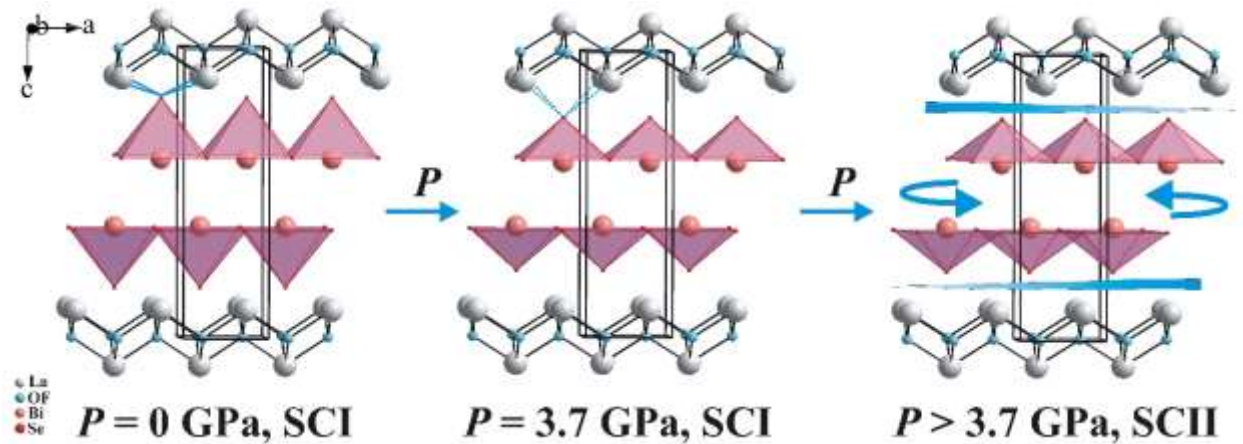


Fig. 1. P -induced evolution of the SCI phase and formation of the SCII phase of $\text{LaO}_{1-x}\text{F}_x\text{BiSe}_2$.

reported to crystallize in a monoclinic structure ($P2_1/m$), as concluded from P -dependent powder diffraction data.²⁰ The proposed HP model for the SCII phase does not, however, satisfactorily fit experimental data ($R_{\text{wp}} = 25,5\%$).²⁰ Interestingly, for certain BiCh_2 -based phases superconducting response at ambient pressure can be enhanced in a similar way as for SCII phases by using a HP annealing technique²²⁻²⁶ and this phenomena was reported to be related to the induced microstructural changes along the c axis, in particular manifested through a peak broadening. Similar broadening was observed for the SCII phase.²⁰ Clearly, detailed P -dependent structural studies on BiCh_2 -based materials are needed to reveal formation mechanism and nature of the SCII phase in order to better understand the associated improvement in superconducting performance. Here we report single crystal synchrotron radiation diffraction studies on $\text{LaO}_{1-x}\text{F}_x\text{BiSe}_2$ and $\text{LaO}_{1-x}\text{F}_x\text{BiS}_2$ compounds as a function of external pressure and temperature. Related *ab initio* calculations have been performed to correlate experimental structural behavior and observed superconducting response at HP.

The $\text{LaO}_{1-x}\text{F}_x\text{BiSe}_2$ and $\text{LaO}_{1-x}\text{F}_x\text{BiS}_2$ monocrystalline samples have been grown by flux method using powders of La_2O_3 , LaF_3 , and Se/S , and metallic La. The exact chemical compositions, as obtained from EDS analysis, are $\text{LaO}_{0.76(1)}\text{F}_{0.24(1)}\text{BiSe}_2$ and $\text{LaO}_{0.68(2)}\text{F}_{0.32(2)}\text{BiS}_2$ with corresponding T_c of 2.6 and 3 K, respectively. P - and T -dependent synchrotron radiation diffraction data were collected at the ID27 HP Beamline, ESRF, Grenoble, using diamond anvil cells to generate HP. More details on synthesis, data collection and analysis are available in Supporting Information.

Reciprocal spaces of the SCI phase for both $\text{LaO}_{1-x}\text{F}_x\text{BiSe}_2$ and $\text{LaO}_{1-x}\text{F}_x\text{BiS}_2$ exhibit regular features fully compatible with a $P4/nmm$ CeBiOS_2 -type structure (Fig. 2, left, Fig. 3, top). No reflections related to a ferro-lattice-distortions observed in²⁷ for $\text{LaO}_{1-x}\text{F}_x\text{BiS}_2$ are present in the SCI phase of $\text{LaO}_{1-x}\text{F}_x\text{BiSe}_2$ and $\text{LaO}_{1-x}\text{F}_x\text{BiS}_2$. The SCI-SCII transition in the $\text{LaO}_{1-x}\text{F}_x\text{BiSe}_2$ sample occurred between 3.7 and 4.8 GPa (data for SCII taken at 5.9 GPa are shown on Fig. 2, right). The most striking difference between the SCI and SCII phases is a change in the nature of

interactions along the c axis, direction of stacking of the BiSe_2 and $\text{LaO}_{1-x}\text{F}_x$ layers (Fig. 1). This is evident from the appearance of diffuse scattering propagating along the c^* direction concomitant with a smearing of the corresponding Bragg reflections (Fig. 2, right bottom; Fig. 3, bottom) which, for layered systems, is indicative of a presence of stacking faults.^{28,29}

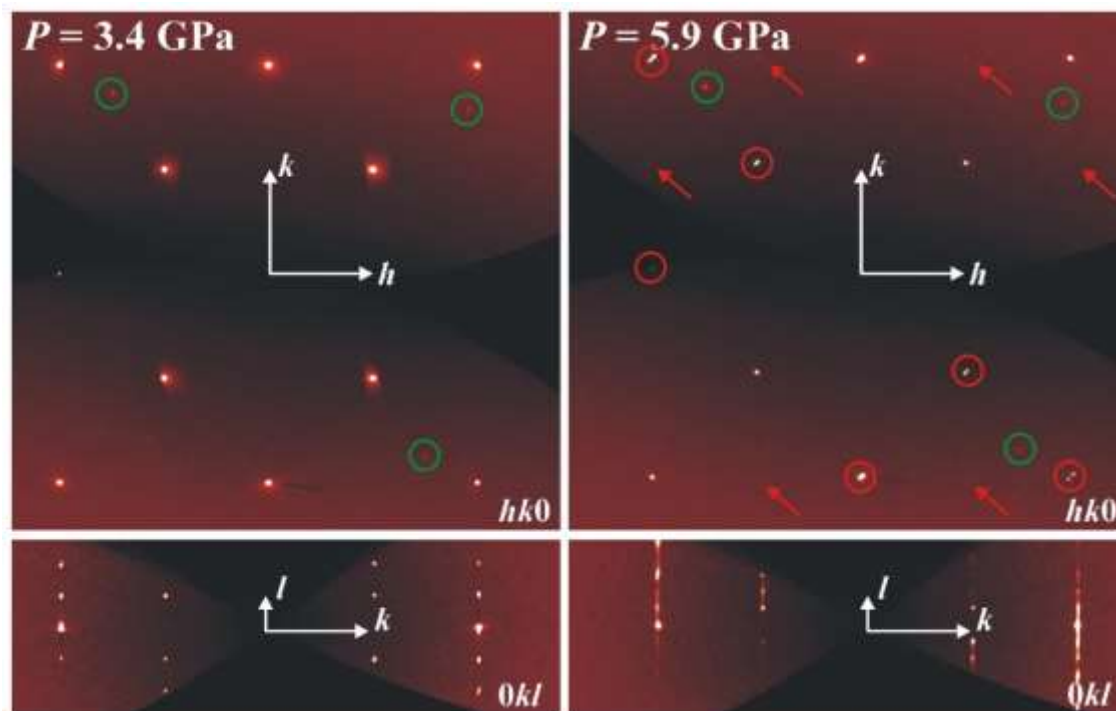


Fig. 2. Slices of the reciprocal space of $\text{LaO}_{1-x}\text{F}_x\text{BiSe}_2$ before (left, SCI phase) and after the P -induced transition (right, SCII phase). Reflections marked with green circles are not commensurate with the reciprocal lattice of $\text{LaO}_{1-x}\text{F}_x\text{BiSe}_2$ and originate from sample environment (diamonds, ruby spheres).

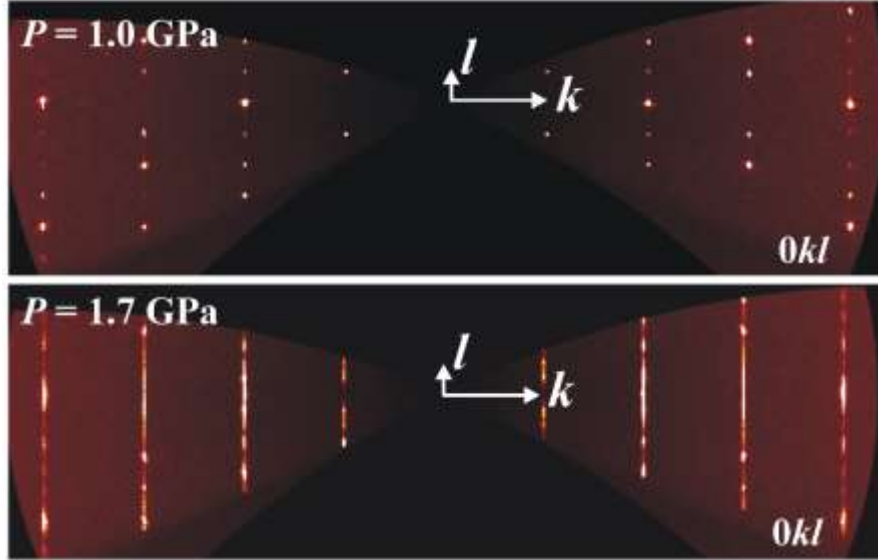


Fig. 3. Slices of the reciprocal space of $\text{LaO}_{1-x}\text{F}_x\text{BiS}_2$ before (top, SCI phase) and after the P -induced transition (bottom, SCII phase).

Structural response of $\text{LaO}_{1-x}\text{F}_x\text{Bi}(\text{Se}/\text{S})_2$ to the application of HP is highly anisotropic, as concluded from single crystal diffraction data for $\text{LaO}_{1-x}\text{F}_x\text{BiSe}_2$. Firstly, while the a and c structural parameters of SCI $\text{LaO}_{1-x}\text{F}_x\text{BiSe}_2$ decrease upon application of pressure (Fig. 4, red and blue curves), a corresponding a/c ratio increases (Fig. 4, black curve). This indicates that relatively to a monotonic decrease along the c direction structure expands in the ab plane.

Atomic parameters of $\text{LaO}_{1-x}\text{F}_x\text{BiSe}_2$ also exhibit a strong anisotropy upon compression. The biggest change is observed for the Bi-Se2 distances which rapidly shrink as a function of pressure (Fig. 5, red lines). The relative decrease is equal to $\sim 12\%$ and results in a flattening of the BiSe_5 pyramids (Fig. 1, middle, the shown amplitude of the flattening is exaggerated for illustration purposes). Interestingly, the La-Se2 distances which correspond to the BiSe_2 -LaO/F interlayer interaction increase with pressure (Fig. 5, black lines), thus these bonds exhibit negative linear compressibility. The resulting weakening in the interlayer bonding yields a strong reduction in a long range crystalline order along the c axis with a subsequent phenomenon of stacking faults (Fig. 1, right) with an associated appearance of diffuse scattering in the reciprocal space. The latter is in the origin of the peak broadening observed on P -dependent powder diffraction data for SCII phase.²⁰ The BiSe_2 and LaO/F layers stay rather rigid in the ab plane and the corresponding bonding exhibits gradual compression with a much smaller relative changes of $<3\%$ for La-O/F (Fig. 5, green lines) and $\sim 1\%$ for Bi-Se1 distances (Fig. 5, blue lines). Results of structural refinement for all the datapoints presented on Figs. 4 and 5 are available in Supporting Information.

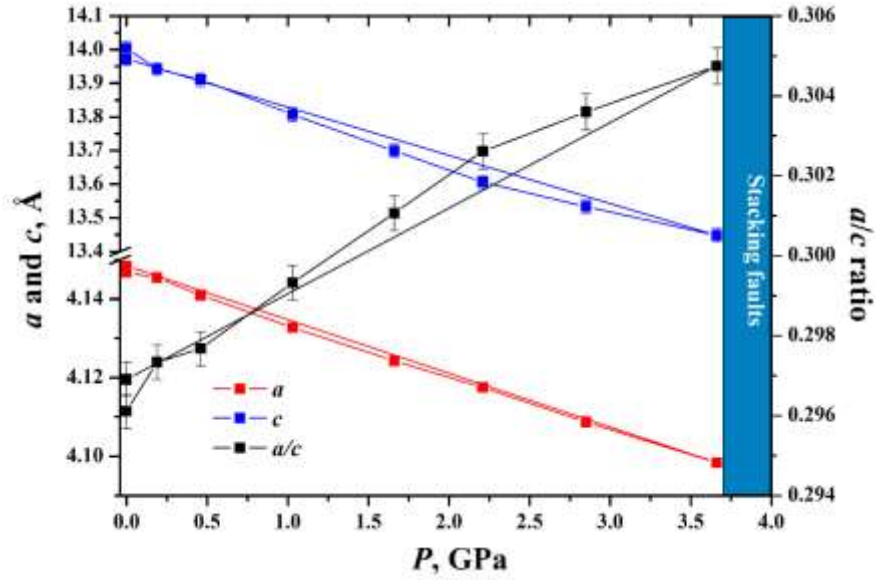


Fig. 4. P -dependent behavior of the a and c parameters of SCI $\text{LaO}_{1-x}\text{F}_x\text{BiSe}_2$ and a corresponding a/c ratio.

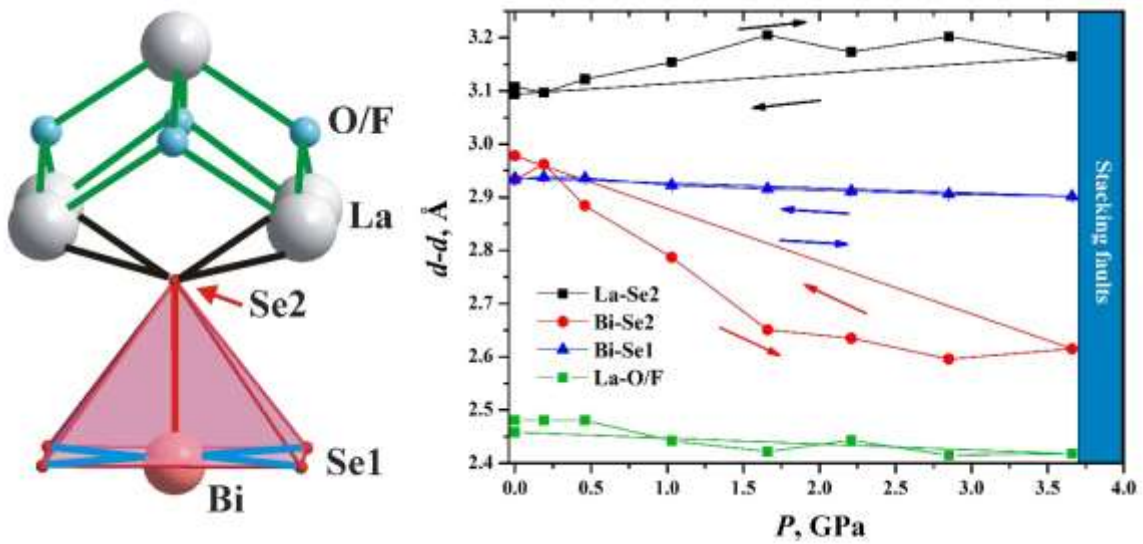


Fig. 5. Bonding evolution in $\text{LaO}_{1-x}\text{F}_x\text{BiSe}_2$ as a function of pressure.

Another interesting feature in the reciprocal space of SCII $\text{LaO}_{1-x}\text{F}_x\text{BiSe}_2$ is a splitting of Bragg reflections (Fig. 2, top right, marked with red circles). This twinning originates from the tetragonal-orthorhombic symmetry lowering associated with the SCI-SCII structural transformation. Two orthorhombic domains of the SCII phase are rotated by $\sim 1.8^\circ$ with respect to

each other and the corresponding orthorhombic distortion increases with pressure (Fig. 6, left). Even though the diffuse scattering along the c^* direction emerges by the expense of intensities of the corresponding Bragg peaks it was still possible to track positions for many of the parent peaks from the collected high resolution single crystal diffraction data. At the SCI-SCII transition point the c parameter, which corresponds to the direction of the stacking, features a decrease of 5.5% with a resulting reduction by 5% in the unit-cell volume (Fig. 6, right). These abrupt changes in structural parameters are characteristic of first-order structural transition. Experimental equations of states (EOS) for the SCI and SCII phases were obtained by fitting the corresponding V - P dependences with Murnaghan (Eq. 1) and 3rd order Birch-Murnaghan (Eq. 2) equations, correspondingly (Table 1). Here V_0 - zero pressure volumes, B_0 - bulk moduli and B_0' - their first pressure derivatives. The SCII is less compressible than the parent low pressure SCI phase and the corresponding zero pressure volume, V_0 , is diminished by ~4%.

$$V(P) = V_0 \left(1 + B_0' \frac{P}{B_0}\right)^{-\frac{1}{B_0}} \quad \text{Eq. 1}$$

$$P(V) = \frac{3B_0}{2} \left[\left(\frac{V_0}{V}\right)^{\frac{7}{3}} - \left(\frac{V_0}{V}\right)^{\frac{5}{3}} \right] \left\{ 1 + \frac{3}{4} (B_0' - 4) \left[\left(\frac{V_0}{V}\right)^{\frac{2}{3}} - 1 \right] \right\} \quad \text{Eq. 2}$$

Table 2. Coefficients of the Murnaghan and 3rd order Birch-Murnaghan EOS for the SCI and SCII phases of $\text{LaO}_{1-x}\text{F}_x\text{BiSe}_2$, respectively.

Phase	$V_0, \text{\AA}^3$	B_0, GPa	B_0', GPa
$\text{LaO}_{1-x}\text{F}_x\text{BiSe}_2$ SCI	241.5(3)	44(5)	8(3)
$\text{LaO}_{1-x}\text{F}_x\text{BiSe}_2$ SCII	231.3(7)	67(3)	4.3(2)

Another difference between the SCII and SCI phases, in addition to the presence of stacking faults and the symmetry lowering, is the presence of new weak reflections with odd $h+k$ indexes which violate the n glide plane of the parent $P4/nmm$ symmetry (Fig. 2, top right, marked with red arrows). The actual space group cannot be assigned for the SCII structure due to a lack of long-range correlations along the c stacking direction. The new $hk0$ pattern is, however, compatible with a model proposed in ²⁷ featuring ferro-lattice-distortions.

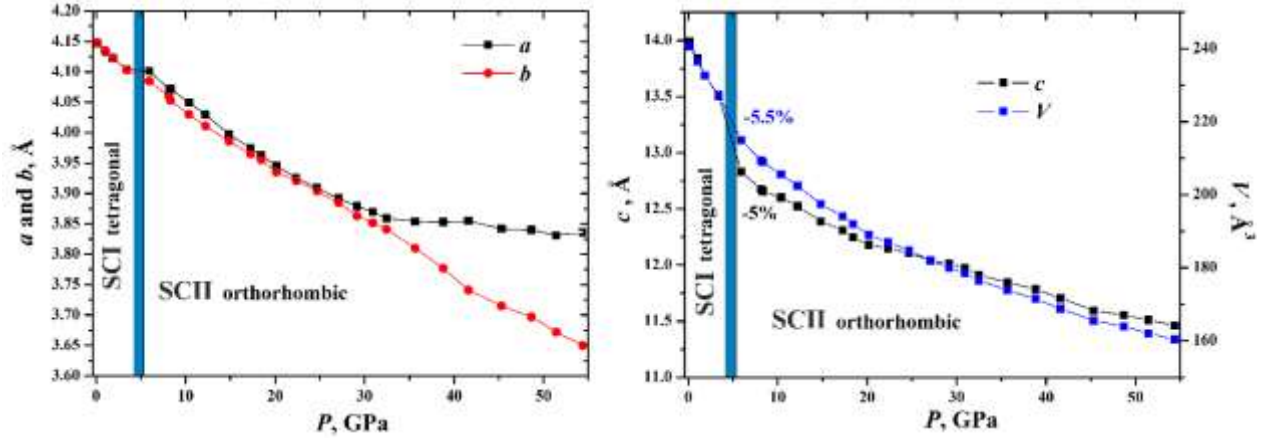


Fig. 6. P -dependent behavior of the a , b (left), c (right) structural parameters and unit-cell volume (right) of $\text{LaO}_{1-x}\text{F}_x\text{BiSe}_2$ up to $P = 55$ GPa.

Although structure of the diffuse rods of $\text{LaO}_{1-x}\text{F}_x\text{BiSe}_2$ is not regular (Fig. 2, bottom right), new intensity maximums with $q = 0.5c^*$ are clearly visible and some of those have even higher intensities than the parent $q = 1c^*$ reflections. This indicates that in addition to original ($q = 1c^*$) correlations of the parent SCI phase new correlations, which correspond to the doubling of the c parameter of the SCI phase ($q = 0.5c^*$), emerge. A corresponding stacking model could comprise BiS_2 layers rotated alternatively clockwise and counterclockwise with respect to the reference LaO/F framework. Interestingly, the $\text{LaO}_{1-x}\text{F}_x\text{BiSe}_2$ phase features much more homogenous structure of the diffuse rods (Fig. 3, bottom) indicating that the corresponding correlations are mostly of a short range order. In addition, the SCI-SCII transition for the BiS_2 -based phase occurs between 1.0 and 1.7 GPa, which is lower than the corresponding transition pressure in $\text{LaO}_{1-x}\text{F}_x\text{BiSe}_2$. Therefore the interlayer $\text{BiS}_2 - \text{LaO/F}$ bonding is weaker compared to the corresponding interactions in the BiSe_2 -based phase. We would like to stress that the framework of the SCII phase of both $\text{LaO}_{1-x}\text{F}_x\text{BiSe}_2$ and $\text{LaO}_{1-x}\text{F}_x\text{BiSe}_2$ is metrically orthorhombic ($\alpha = \beta = \gamma = 90^\circ$) and therefore the monoclinic $P2_1/m$ symmetry with $\beta = 97.3^\circ$ proposed in²⁰ is not compatible with our data.

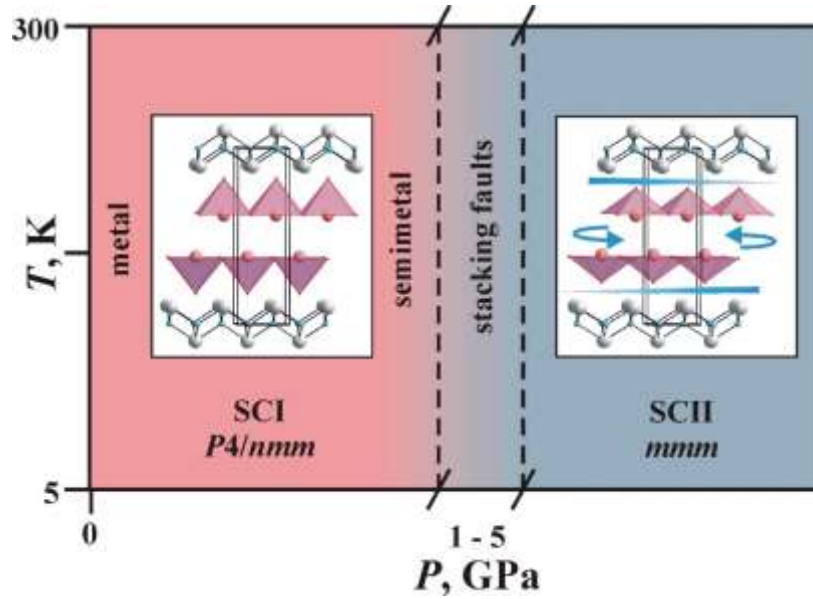


Fig. 7. Schematic T - P phase diagram of $\text{LaO}_{1-x}\text{F}_x\text{BiSe}_2$ and $\text{LaO}_{1-x}\text{F}_x\text{BiS}_2$. The Laue mmm class is indicated for the orthorhombic SCII phase.

At ambient temperature the SCI-SCII transition is reversible, i.e. diffuse rods disappear upon decompression. Nevertheless, the HP annealing likely stabilizes the SCII phase which is manifested through a broadening of reflections on experimental powder diffraction data.²²⁻²⁶ Single crystal diffraction experiments at HP-HT conditions are needed to confirm this likely scenario. Finally, compression at 5 K was performed to study phase behavior for both $\text{LaO}_{1-x}\text{F}_x\text{BiSe}_2$ and $\text{LaO}_{1-x}\text{F}_x\text{BiS}_2$ at superconducting conditions. At 5 K the SCI-SCII transition in $\text{LaO}_{1-x}\text{F}_x\text{BiSe}_2$ occurred between 2.9 and 5.2 GPa, i.e. in the same pressure range as at ambient temperature. Similarly, the $\text{LaO}_{1-x}\text{F}_x\text{BiS}_2$ sample transitioned already at 1.7 GPa (the first pressure point collected at 5 K). Thus the SCI-SCII phase boundary in a T - P space is rather vertical for both $\text{LaO}_{1-x}\text{F}_x\text{BiSe}_2$ and $\text{LaO}_{1-x}\text{F}_x\text{BiS}_2$ and the corresponding phase diagram is shown in Fig. 7.

Electronic density of states (DOS) have been calculated for $\text{LaO}_{1-x}\text{F}_x\text{BiSe}_2$ structures at 0 and 3.7 GPa, right before the onset of the SCI-SCII transition, in order to deduce the electronic origin of the decrease in T_c observed experimentally in this phase as a function of pressure.^{6,7} Calculations were performed with a Wien2k 18.2 code³⁰ using the PBE-GGA exchange correlation potential.³¹ The Brillouin zone (BZ) was divided with a k-mesh of 784 points (56 k-points in the irreducible region of the BZ). For each pressure structural parameters obtained from the corresponding diffraction data were used; O/F atomic position was considered as fully occupied solely by oxygen atoms ($x = 0$).

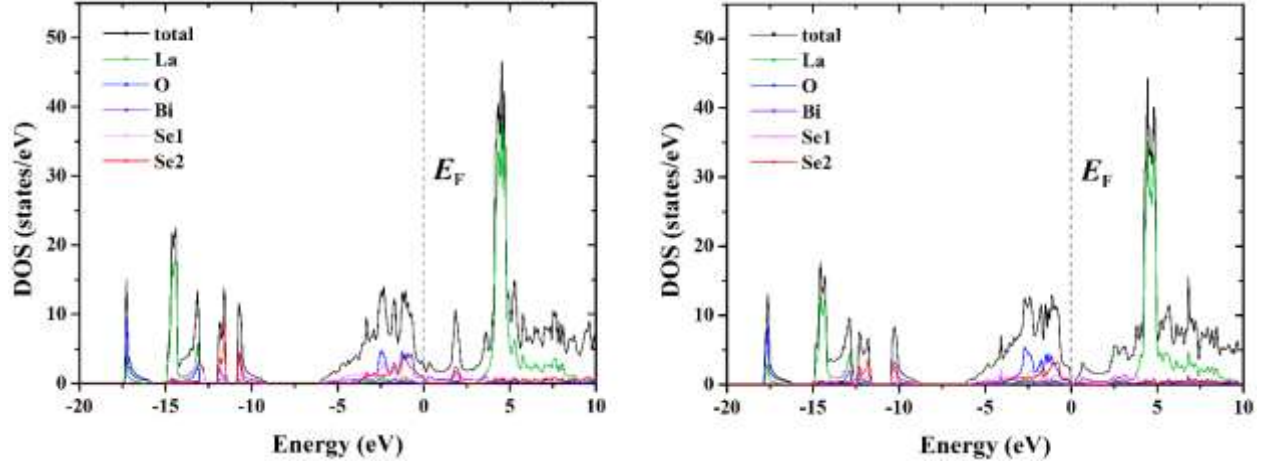


Fig. 8. Calculated DOS for the $\text{LaO}_{1-x}\text{F}_x\text{BiSe}_2$ structures at 0 (left) and 3.7 GPa (right).

At ambient pressure the electronic states of $\text{LaO}_{1-x}\text{F}_x\text{BiSe}_2$ ($x = 0$) at the Fermi level, E_F , are populated essentially by p -levels of Se2 and O atoms (Fig. 8, left, red and blue curves) indicating a presence of an inter-layer charge transfer, similarly to the $\text{LaO}_{1-x}\text{F}_x\text{BiS}_2$ system.³² Electron doping by partial substitution of F for O directly replenishes electronic states at E_F therefore enhancing metallic properties of the parent LaOBiSe_2 phase. Contrary, application of HP nearly depletes electronic states at E_F with a complete depletion right above E_F producing a small bandgap of 0.04 eV (Fig. 8, right). The resulting semimetallic behavior is associated with a decrease in T_c for this phase. However, the following SCI-SCII transition enhances two-dimensionality in $\text{LaO}_{1-x}\text{F}_x\text{BiSe}_2$, as demonstrated above, resulting in a phase with superior superconducting properties.

In summary, HP drastically enhances two-dimensionality in $\text{LaO}_{1-x}\text{F}_x\text{Bi}(\text{Se}/\text{S})_2$. The associated reduction in long-range order along the direction of stacking of $\text{Bi}(\text{Se}/\text{S})_2$ and LaO/F layers induces formation of stacking faults. The HP SCII $\text{LaO}_{1-x}\text{F}_x\text{BiSe}_2$ phase better preserves long-range order of the parent SCI phase compared to the S-containing one. This is evident from a more homogeneous structure of diffuse rods for $\text{LaO}_{1-x}\text{F}_x\text{BiS}_2$ and, therefore, this system is characterized by weaker interlayer interactions which results in lower SCI-SCII transition pressure. Studied $\text{LaO}_{1-x}\text{F}_x\text{Bi}(\text{Se}/\text{S})_2$ systems illustrate how structural two-dimensionality is critical for layered superconductors. Targeted enhancement of 2D-structure of layered systems either by external (pressure, temperature) or internal (chemical doping, substitutions) means should be considered as another pathway to further improve their superconducting performance.

Acknowledgments

This work was also partly supported by statutory budget of Faculty of Chemistry, Warsaw University of Technology.

References

- (1) Mizuguchi, Y.; Fujihisa, H.; Gotoh, Y.; Suzuki, K.; Usui, H.; Kuroki, K.; Demura, S.; Takano, Y.; Izawa, H.; Miura, O. *Phys. Rev. B* **2012**, *86*, 220510.
- (2) Singh, S. K.; Kumar, A.; Gahtori, B.; Shruti; Sharma, G.; Patnaik, S.; Awana, V. P. S. *J. Am. Chem. Soc.* **2012**, *134*, 16504.
- (3) Mizuguchi, Y. *J. Phys. Soc. Japan* **2019**, *88*, 041001.
- (4) Ruan, B.-B.; Zhao, K.; Mu, Q.-G.; Pan, B.-J.; Liu, T.; Yang, H.-X.; Li, J.-Q.; Chen, G.-F.; Ren, Z.-A. *J. Am. Chem. Soc.* **2019**, *141*, 3404.
- (5) Krzton-Maziopa, A.; Guguchia, Z.; Pomjakushina, E.; Pomjakushin, V.; Khasanov, R.; Luetkens, H.; Biswas, P. K.; Amato, A.; Keller, H.; Conder, K. *J. Phys.: Cond. Matt.* **2014**, *26*, 215702.
- (6) Liu, J.; Li, S.; Li, Y.; Zhu, X.; Wen, H.-H. *Phys. Rev. B* **2014**, *90*, 094507.
- (7) Jha, R.; Awana, V. P. S. *J. Supercond. Nov. Magn.* **2015**, *28*, 2229.
- (8) Fujioka, M.; Tanaka, M.; Denholme, S. J.; Yamaki, T.; Takeya, H.; Yamaguchi, T.; Takano, Y. *EPL* **2014**, *108*, 47007.
- (9) Tanaka, M.; Nagao, M.; Matsumoto, R.; Kataoka, N.; Ueta, I.; Tanaka, H.; Watauchi, S.; Tanaka, I.; Takano, Y. *J. Alloys Compd.* **2017**, *722*, 467.
- (10) Wolowiec, C. T.; White, B. D.; Jeon, I.; Yazici, D.; Huang, K.; Maple, M. B. *J. Phys.: Cond. Matt.* **2013**, *25*, 422201.
- (11) Fujioka, M.; Nagao, M.; Denholme, S. J.; Tanaka, M.; Takeya, H.; Yamaguchi, T.; Takano, Y. *Appl. Phys. Lett.* **2014**, *105*, 052601.
- (12) Guo, C. Y.; Chen, Y.; Smidman, M.; Chen, S. A.; Jiang, W. B.; Zhai, H. F.; Wang, Y. F.; Cao, G. H.; Chen, J. M.; Lu, X.; Yuan, H. Q. *Phys. Rev. B* **2015**, *91*, 214512.
- (13) Thakur, G. S.; Jha, R.; Haque, Z.; Awana, V. P. S.; Gupta, L. C.; Ganguli, A. K. *Supercond. Sci. Tech.* **2015**, *28*, 115010.
- (14) Luo, Y.; Zhai, H.-F.; Zhang, P.; Xu, Z.-A.; Cao, G.-H.; Thompson, J. D. *Phys. Rev. B* **2014**, *90*, 220510.
- (15) Fang, Y.; Yazici, D.; Jeon, I.; Maple, M. B. *Phys. Rev. B* **2017**, *96*, 214505.
- (16) Fang, Y.; Yazici, D.; White, B. D.; Maple, M. B. *Phys. Rev. B* **2015**, *92*, 094507.
- (17) Kalai Selvan, G.; Thakur, G. S.; Manikandan, K.; Banerjee, A.; Haque, Z.; Gupta, L. C.; Ganguli, A. K.; Arumugam, S. *J. Phys. D: Appl. Phys.* **2016**, *49*, 275002.
- (18) Jha, R.; Kishan, H.; Awana, V. P. S. *J. Phys. Chem. Solids* **2015**, *84*, 17.
- (19) Wolowiec, C. T.; Yazici, D.; White, B. D.; Huang, K.; Maple, M. B. *Phys. Rev. B* **2013**, *88*, 064503.
- (20) Tomita, T.; Ebata, M.; Soeda, H.; Takahashi, H.; Fujihisa, H.; Gotoh, Y.; Mizuguchi, Y.; Izawa, H.; Miura, O.; Demura, S.; Deguchi, K.; Takano, Y. *J. Phys. Soc. Japan* **2014**, *83*, 063704.
- (21) Fang, Y.; Wolowiec, C. T.; Breindel, A. J.; Yazici, D.; Ho, P. C.; Maple, M. B. *Supercond. Sci. Tech.* **2017**, *30*, 115004.
- (22) Kajitani, J.; Hiroi, T.; Omachi, A.; Miura, O.; Mizuguchi, Y. *J. Supercond. Nov. Magn.* **2015**, *28*, 1129.
- (23) Deguchi, K.; Mizuguchi, Y.; Demura, S.; Hara, H.; Watanabe, T.; Denholme, S. J.; Fujioka, M.; Okazaki, H.; Ozaki, T.; Takeya, H.; Yamaguchi, T.; Miura, O.; Takano, Y. *EPL* **2013**, *101*, 17004.

- (24) Pallecchi, I.; Lamura, G.; Putti, M.; Kajitani, J.; Mizuguchi, Y.; Miura, O.; Demura, S.; Deguchi, K.; Takano, Y. *Phys. Rev. B* **2014**, *89*, 214513.
- (25) Kajitani, J.; Deguchi, K.; Omachi, A.; Hiroi, T.; Takano, Y.; Takatsu, H.; Kadowaki, H.; Miura, O.; Mizuguchi, Y. *Solid State Commun.* **2014**, *181*, 1.
- (26) Kajitani, J.; Deguchi, K.; Hiroi, T.; Omachi, A.; Demura, S.; Takano, Y.; Miura, O.; Mizuguchi, Y. *J. Phys. Soc. Japan* **2014**, *83*, 065002.
- (27) Athauda, A.; Hoffmann, C.; Aswartham, S.; Terzic, J.; Cao, G.; Zhu, X.; Ren, Y.; Louca, D. *J. Phys. Soc. Japan* **2017**, *86*, 054701.
- (28) Svitlyk, V.; Campbell, B. J.; Mozharivskyj, Y. *Inorg. Chem.* **2009**, *48*, 10364.
- (29) Svitlyk, V.; Cheung, J. Y. Y.; Mozharivskyj, Y. *J. Magn. Magn. Mater.* **2010**, *322*, 2558.
- (30) Blaha, P.; Schwarz, K.; Madsen, G. K. H.; Kvasnicka, D.; Luitz, J.; Laskowski, R.; Tran, F.; Marks, L. D. 2018.
- (31) Perdew, J. P.; Burke, K.; Ernzerhof, M. *Phys. Rev. Lett.* **1996**, *77*, 3865.
- (32) Shein, I. R.; Ivanovskii, A. L. *JETP Lett.* **2013**, *96*, 769.